



# 1 **Gains and losses in surface solar radiation with dynamic** 2 **aerosols in regional climate simulations for Europe**

3 Sonia Jerez<sup>1\*</sup>, Laura Palacios-Peña<sup>1</sup>, Claudia Gutiérrez<sup>2</sup>, Pedro Jiménez-Guerrero<sup>1</sup>, Jose María  
4 López-Romero<sup>1</sup>, Juan Pedro Montávez<sup>1</sup>

5 (1) Regional Atmospheric Modeling (MAR) group, Department of Physics, University of Murcia,  
6 30100 Murcia, Spain

7 (2) Environmental Sciences Institute, University of Castilla-La Mancha, 45071 Toledo, Spain

8 \*Correspondence to: [sonia.jerez@gmail.com](mailto:sonia.jerez@gmail.com)

## 9 **Abstract**

10 The solar resource can be highly influenced by clouds and atmospheric aerosol, which has been  
11 named by the IPCC as the most uncertainty climate forcing agent. Nonetheless, Regional Climate  
12 Models (RCMs) hardly ever model dynamically atmospheric aerosol concentration and their  
13 interaction with radiation and clouds, in contrast to Global Circulation Models (GCMs). The  
14 objective of this work is to evince the role of the interactively modeling of aerosol concentrations  
15 and their interactions with radiation and clouds in Weather Research and Forecast (WRF) model  
16 simulations with a focus on summer mean surface downward solar radiation (RSDS) and over  
17 Europe. The results show that the response of RSDS is mainly led by the aerosol effects on  
18 cloudiness, which explain well the differences between the experiments in which aerosol-radiation  
19 and aerosol-radiation-cloud interactions are taken into account or not. Under present climate, a  
20 reduction about 5% in RSDS was found when aerosols are dynamically solved by the RCM, which  
21 is larger when only aerosol-radiation interactions are considered. However, for future projections,  
22 the inclusion of aerosol-radiation-cloud interactions results in the most negative RSDS change  
23 pattern (while with slight values), showing noticeable differences with the projections from either  
24 the other RCM experiments or from their driving GCM (which do hold some significant positive  
25 signals). Differences in RSDS among experiments are much more softer under clear-sky conditions.



## 26 **1 – Introduction**

27 Regional Climate Models (RCMs) are powerful tools providing high resolution climate information  
28 by dynamically downscaling coarser datasets, e.g. from Global Circulation Models (GCMs). Their  
29 added value is not only about the increased resolution, but also about the fact that such an increased  
30 resolution allows modeling and considering fine scale processes and features that are missed or  
31 misrepresented otherwise, e.g. local circulations and land uses (Rummukainen 2010, Jacob et al  
32 2014, 2020, Schewe et al 2019). Still, certain phenomena need to be parametrized, e.g. the  
33 turbulence within the planetary boundary layer, the microphysics processes and all about cumulus.  
34 However, there are relevant processes that GCMs usually model dynamically, but RCMs usually do  
35 not. This is the case of the atmospheric aerosols concentration and their multiple non-linear  
36 interactions (eg. Taylor et al 2012 vs. Ruti et al 2016), the so-called aerosol-radiation and aerosol-  
37 cloud interactions (Boucher 2015).

38 Depending on their nature and on the ambient conditions, aerosols can act to scatter and/or absorb  
39 the solar radiation, which may result on less or more solar radiation reaching the surface; less  
40 because of its scattering (direct effect), more if absorption (semi-direct effect) leads to clouds burn-  
41 off and/or inhibition (Giorgi et al 2002, Nabat et al 2015a, Li et al 2017, Kinne 2019). Aerosols also  
42 act as cloud condensation nuclei (indirect effect), which may also result on less or more solar  
43 radiation reaching the surface. Abundance of cloud condensation nuclei rebounds on enhanced  
44 scattering by whitened clouds of smaller drops with increased size and lifetime, and on the drizzle  
45 suppression which reduces bellow-cloud wet deposition processes (Seinfeld et al 2016, Kinne  
46 2019). Contrary, in-cloud aerosol scavenging processes lead to out-of-clouds cleaner atmospheres  
47 (Croft et al 2012). All these processes have the potential to alter local and regional circulations,  
48 therefore impacting beyond the radiative balance (Kloster et al 2010, Wilcox et al 2013, Nabat et al  
49 2014, Wang et al 2016, Pavlidis et al 2020).

50 In the current context of climatic crisis, the scientific challenge is getting twofold: (1) a good  
51 understanding of processes that occur in the atmosphere and of what will occur in the future,  
52 because this is crucial (IPCC 2013) in order to (2) advance effective measures both at global and  
53 regional scales (IPCC 2014). In particular, climate change mitigation strategies require that low-  
54 carbon energies grow very fast in the coming decades (Rohrig et al 2019, IRENA 2019). This rapid  
55 transition of the energy sector towards renewables-powered decarbonized systems makes the energy  
56 production, transmission and distribution increasingly sensitive to weather and climate variability



57 (Jerez et al 2013, Bloomfield et al 2016, Collins et al 2018, Kozarcenin et al 2018, Troccoli et al  
58 2018, Germer & Kleidon 2019, Turner et al 2019, van der Wiel et al 2019, van Ruijven et al 2019).  
59 Thus, several works have been devoted to assess this issue through the use of climate modelling  
60 tools (Crook et al 2011, Gaetani et al 2014, Jerez et al 2015, Tobin et al 2015, Wild et al 2015,  
61 Tobin et al 2016, Bartók et al 2017, Tobin et al 2018, Ravestein et al 2018, Schlott et al 2018, Gil et  
62 al 2019, Jerez et al 2019, Müller et al 2019, Soares et al 2019, Solaun & Cerdá 2019, Zappa et al  
63 2019).

64 From the extensive literature, we rescue here four key features that motivated the present work.  
65 First, the increasing use of RCM to perform evaluations of the renewable energy resources and their  
66 supplying potential (e.g. Jerez et al 2013, 2015, 2019, Tobin et al 2015, 2016, Gil et al 2019, Soares  
67 et al 2019). Second, the key role of aerosols regarding the accuracy of the simulated solar resource  
68 by climate models (Gaetani et al 2014, Nabat et al 2015b, Gutiérrez et al 2018, 2020, Boé et al  
69 2020, Pavlidis et al 2020). Third, the reported discrepancies between GCMs and RCMs future  
70 projections for the solar resource (Jerez et al 2015, Bartók et al 2017), which still remain largely a  
71 mystery. And fourth, none of the previous studies has unveiled so far the non-evident role of  
72 interactively modeled atmospheric aerosol concentrations and the resulting aerosol-radiation and  
73 aerosol-cloud interactions for simulating the solar resource using regional climate models under  
74 present and future climate scenarios.

75 Hence, our objective here is to shed light on that. For that, we made use of a widely applied RCM,  
76 the Weather Research and Forecasting (WRF) Model (Skamarock et al 2008) and its coupled form  
77 with Chemistry (WRF-Chem; Grell et al 2005), to perform sets of present (period 1991-2010) and  
78 future (period 2031-2050) simulations over Europe in three ways: (1) without dynamic aerosol  
79 modeling, (2) with dynamic aerosols and aerosol-radiation interactions activated, and (3) with  
80 dynamic aerosols and both aerosol-radiation and aerosol-cloud interactions activated.

81 Section 2 provides experimental details. Section 3 presents the results. Conclusions are drawn and  
82 discussed in Section 4.



## 83 2 – Experiments and data

84 We performed three experiments using the WRF model version 3.6.1 (Skamarock et al 2008;  
85 available at <https://www.mmm.ucar.edu/weather-research-and-forecasting-model>, last accessed on  
86 2019-11-28). In all cases, the simulated periods were 1991-2010 (present) and 2031-2050 (future).  
87 Initial and boundary conditions were taken from GCM simulations: the r1i1p1 MPI-ESM-LR  
88 historical and RCP8.5-forced runs (Giorgetta et al. 2012a,b; available at <https://cera-www.dkrz.de>,  
89 last accessed on 2019-11-28) from the Coupled Model Intercomparison Project Phase 5 (CMIP5;  
90 <https://pcmdi.llnl.gov/mips/cmip5/>; Taylor et al 2012). The Representative Concentration Pathway  
91 RCP8.5 (Moss et al 2010) depicts the highest radiative forcing along the XXI century among all  
92 RCPs, with doubled CO<sub>2</sub>, CH<sub>4</sub>, and N<sub>2</sub>O concentrations by 2050 compared to the last record of the  
93 historical period. Both the observed (past) and estimated (future) temporal evolution of the  
94 concentration of these species was appropriately considered in the WRF executions (Jerez et al  
95 2018).

96 The three experiments consisted of, and are named as:

97 BASE: aerosols are not treated interactively, the by-default WRF setup was used, which considers  
98 250 cloud condensation nuclei per cm<sup>3</sup> to form clouds, and the aerosol radiative effect is assumed to  
99 come as an external forcing.

100 ARI: aerosols are treated interactively (see bellow) and aerosol-radiation interactions are activated  
101 in the model.

102 ACI: aerosols are treated interactively, as in ARI experiments, and both aerosol-radiation and  
103 aerosol-cloud interactions are activated in the model.

104 The WRF spatial configuration consisted of two one-way nested domains (Supp Fig 1). The inner  
105 one (target domain) is an Euro-Cordex (<https://www.euro-cordex.net/>; Jacob et al 2014, 2020)  
106 compliant domain covering Europe with an horizontal resolution of 0.44° in latitude and longitude.  
107 The outer one has a horizontal resolution of 1.32° and covers the most important areas of Saharan  
108 dust emission as in Palacios-Peña et al 2019a. This configuration was necessary to generate and  
109 include the information of the Saharan dust intrusions through the boundaries of our target domain  
110 for the ARI and ACI experiments, because the boundary conditions from the GCM do not provide



111 this information. In the vertical dimension, 29 unevenly spaced eta levels were specified in the two  
112 domains, with more levels near the surface than upward, and the model top was set to 50 hPa. The  
113 physics configuration of the WRF model consisted of the Lin microphysics scheme (Lin et al.  
114 1983), the RRTM radiative scheme (Iacono et al. 2008), the Grell 3D ensemble cumulus scheme  
115 (Grell 1993, Grell and Dévényi 2002), the University of Yonsei boundary layer scheme (Hong et al.  
116 2006) and the Noah land surface model (Chen & Dudhia 2001, Tewari et al. 2004). Boundary  
117 conditions from the GCM were updated every 6 hours, including the low boundary condition for the  
118 sea surface temperature. Nudging was applied to the outer domain, but not to the target domain.

119 To perform ARI and ACI experiments, we used the WRF model coupled with Chemistry (WRF-  
120 Chem) version 3.6.1 (Grell et al 2005, Chin et al 2002). WRF-Chem runs with GOCART aerosol  
121 module (Ginoux et al 2001). This scheme was coupled with RACM-KPP (Stockwell et al 1997,  
122 Geiger et al 2003) as chemistry option. The Fast-J module (Wild et al 2000) was used as photolysis  
123 option. Biogenic emissions were calculated using the Guenther scheme (Guenther et al 2006). The  
124 simulated aerosols included five species, namely sulphate, mineral dust, sea salt aerosol, organic  
125 matter and black carbon. Anthropogenic emissions coming from the Atmospheric Chemistry and  
126 Climate Model Intercomparison Project (ACCMIP; Lamarque et al 2010) were kept unchanged in  
127 the simulation periods (we considered the 2010 monthly values). Natural emissions depend on  
128 ambient conditions and varied accordingly in our simulations following Ginoux et al 2001 for dust  
129 and Chin et al 2002 for sea salt.

130 The inclusion of aerosol-radiation and aerosol-cloud interactions in ARI and ACI simulations are  
131 extensively described in Palacios-Peña et al 2020. However, a brief summary is included here. The  
132 former (aerosol-radiation) are included following Fast et al 2006 and Chapman et al 2009. The  
133 overall refractive index for a given size bin was determined by volume averaging associating each  
134 chemical constituent of aerosol with a complex index of refraction. The Mie theory and the  
135 summation over all size bins were used to determine the composite aerosol optical properties  
136 assuming wet particle diameters. Finally, aerosol optical properties are transferred to the shortwave  
137 radiation scheme. Aerosol-cloud interactions were implemented by linking the simulated cloud  
138 droplet number with the microphysics schemes (Chapman et al 2009) affecting both the calculated  
139 droplet mean radius and the cloud optical depth. Although this WRF-Chem version (3.6.1) does not  
140 allow a full coupling with aerosol-cloud interactions, the microphysics implemented here is a single  
141 moment scheme that turns into a two moments scheme in the simulations denoted as ACI.



142 The WRF outputs were recorded every hour, in particular for the variables of interest here, namely  
143 Surface Downward Solar Radiation (RSDS) and Total Cloud Cover (CCT). We also compute AOD  
144 at 550 nm from the WRF-Chem outputs following Palacios-Peña et al (2019b).  $RSDS_{cs}$  and  $AOD_{cs}$   
145 will denote the RSDS and AOD values under clear sky conditions, computed here at the daily time  
146 scale from those days with values of CCT lower than 1%. The RSDS and CCT data simulated by  
147 the driving GCM runs were used for comparison purposes. We also retrieved the AOD at 550 nm as  
148 seen by the GCM from the MACv2 data (Kinne et al 2019), whose anthropogenic changes are in  
149 accordance with the RCP8.5 while its coarse mode (of natural origin) was not allowed to change.  
150 Summer (JJA: June-July-August) means of all the variables were used in the analysis. The analysis  
151 involving  $RSDS_{cs}$  and  $AOD_{cs}$  will be considered only over those grid points where at least 75% of  
152 the summer mean values in the time series (i.e. at least 15 records per period) are not missing values  
153 (which, according to our methodology, would occur only if all days within a summer season have  
154 CCT values  $\geq 1\%$ ).

### 155 **3 - Results**

156 We focus on the summer season (JJA), when solar energy provides its most, AOD typically reaches  
157 the highest values and the aerosol radiative effect has been proven to be strongest (Pavlidis et al  
158 2020). As a first test, Supp Fig 2a-d provides the GCM, BASE, ARI and ACI JJA climatologies of  
159 RSDS in the present period. Although the four patterns depict similar structures, a closer look to the  
160 deviations of the climatologies from the WRF experiments with respect to the GCM (Supp Fig 2e-  
161 g) reveals significant differences through resembling patterns: positive values (higher RSDS values  
162 in the RCM experiments) south and northward (up to 20 and 30% respectively), and negative values  
163 in between (10-15%, eventually up to 25%). Nonetheless, there still exist significant differences  
164 within the set of WRF experiments (Fig 1a-c), in which this research puts the focus.

165 The inclusion of interactive aerosols (ARI and ACI experiments) reduce the JJA mean values of  
166 RSDS in central and northern parts of our domain by a few percents as compared to the BASE  
167 experiment (Fig 1a,b). This reduction is generally stronger in ARI than in ACI. Consequently, the  
168 ACI minus ARI pattern (Fig 1c) depicts mostly positive values over central and southern regions. In  
169 order to try to understand these patterns, Fig 1 also provides differences in the CCT and AOD  
170 summer climatologies between experiments and the spatial correlations ( $s_{corr}$ ) between these  
171 patterns and those of RSDS differences (panels d to f and g to i, respectively). Compared to BASE,



172 both ARI and ACI lead to more cloudiness in central and northern regions and less cloudiness  
173 southward, specially in ACI (Fig 1d-f), which is well correlated with the spatial distribution of the  
174 differences between experiments in RSDS. Also, the dynamic treatment of aerosols lead to  
175 noticeable differences (up to 10%) in the AOD values between ACI and ARI (Fig 1i), and the AOD  
176 climatologies from these two experiments provides a consistently non-nule picture (Fig 1g,h; nule  
177 values can be considered for BASE). However, the patterns for AOD do not correlate with those for  
178 RSDS. In fact, the temporal correlation at the grid point level between the series of differences in  
179 RSDS and in CTT is above 0.8 (negative) in most of the domain, while differences in AOD hardly  
180 correlates in time with differences in RSDS (Supp Fig 3a-f). Hence, the CTT differences prevail  
181 over the AOD differences in driving the RSDS differences between pairs of experiments in the  
182 present-day climate simulations. This also holds under future conditions, while the patterns of  
183 differnces in the analyzed variables show different structures (Supp Fig 4 and 5a-f).

184 Therefore, there is an overall a direct and predominant link between the aerosols effect on  
185 cloudiness and its impact on the amount of solar radiation reaching the surface. Contrary, the effect  
186 of interactive aerosols schemes on AOD seems to play a minor and more local role in certain  
187 locations, where it eventually can help to straightly explain the differences in RSDS between ACI  
188 and ARI as the matching between the RSDS and CCT differences devanishes. For instance, a closer  
189 look to local differences between ARI/ACI and BASE reveals regions (in central and eastern  
190 Mediterranean Europe) where, in spite of the less CCT simulated in experiments with interactive  
191 aerosols (Fig 1d,e), they also simulate less RSDS than BASE (Fig 1a,b). This could be explained by  
192 the differences in AOD and its locally relevant impact on RSDS over thse regions, as pointed out by  
193 Supp Fig 3d. Also, over areas of central Europe, while differences between ACI and ARI in CTT  
194 are small (Fig 1f), ACI provides higher values of RSDS than ARI (Fig 1c), which could be  
195 explained by the larger AOD values in the ARI simulation (Fig 1i).

196 Under clear-sky conditions (Fig 2), both the spatial correlations between patterns of AOD and  
197 RSDS differnces, and the temporal correlations between the respective series computed at the grid  
198 point level (Supp Fig 3g-i, 5g-i and 6), support the relevant role of the AOD<sub>cs</sub> variable for the  
199 simulation of RSDS<sub>cs</sub>. Nonetheless, differences in RSDS<sub>cs</sub> are lower than differences in RSDS,  
200 basically nule between ACI and ARI. It is important to note that this analysis considers coincident  
201 clear-sky dates between the pairs of experiment being faced (the percentage of days retained under  
202 this approach can be seen in Supp Fig 7). Without this restriction (see the percentage of days  
203 retained in Supp Fig 8) the match between both variables devanishes both in the present and the



204 future periods (Supp Fig 9 and 10), may indicating the masking effect of Earth orbit related issues,  
205 of large scale climate drivers and/or local forcings such as water vapor content.

206 Cloudiness also seems to lead the future projections for the RSDS summer climatologies (Fig 3).  
207 BASE and ARI change patterns for RSDS (Fig 3b,c) resemble each other, with negative signals (up  
208 to 10%) appearing in northernmost regions while positive signals (up to 5%) appear southward  
209 within our target domain. These latter are more widespread in ARI than in BASE, which makes the  
210 ARI pattern the most similar to the change pattern from the GCM (Fig 3a). However, when  
211 aerosols-cloud interactions are included in the WRF runs, such a positive RSDS change signals  
212 mostly disappear while the northern negative ones reinforce in some parts as compared to the ARI  
213 pattern (Fig 3d). All this is in quite good agreement with the corresponding change patterns for CCT  
214 (Fig 3e-h) – including the fact that the negative change signals for CCT appearing southward in the  
215 GCM, BASE and ARI experiments are way less evident in ACI – and occurs in spite of two  
216 constraining facts regarding the AOD simulation approaches in our WRF experiments: (1) AOD  
217 remains unchanged in the BASE experiment (as illustrated by Fig 3j), and (2) AOD changes from  
218 the ARI and ACI experiments are hardly realistic because their anthropogenic component is  
219 disregarded (as specified in Section 2), and thus depict patterns (Fig 3k,l) that have nothing to do  
220 with the GCM projection in Fig 3i (which does consider time evolving anthropogenic aerosols). In  
221 fact, the spatial correlation between the patterns of AOD and RSDS changes is lower than between  
222 the patterns of CTT and RSDS changes, specially in ACI, the experiment in which aerosols also act  
223 on clouds.

224 The change signals for  $RSDS_{cs}$  and  $AOD_{cs}$  (Fig 4) depict softer and with a different spatial structure  
225 to those for RSDS and AOD in the ARI and ACI experiments, turning mostly negative southward  
226 and positive northward for  $RSDS_{cs}$ , which occurs similarly in the three experiments (BASE, ARI  
227 and ACI). There is no clear relation between  $AOD_{cs}$  change patterns and  $RSDS_{cs}$  changes (low  
228 spatial correlation), except for some local signals in areas at the North-East. However, as discussed  
229 above, the role of retaining, or not, coincident clear-sky dates between pairs of experiments is  
230 important to filter out the true role of  $AOD_{cs}$  on  $RSDS_{cs}$ . Thus, the fact that change patterns are  
231 constructed over different dates may partially explain the apparently negligible role of  $AOD_{cs}$  on  
232  $RSDS_{cs}$  in this case. But only partially, as the BASE change pattern for  $RSDS_{cs}$  (simulated on the  
233 ground of nule  $AOD_{cs}$  change) resemble the respective patterns from ARI and ACI experiments.





#### 234 **4 - Discussion and conclusions**

235 We presented here a research on the role of dynamically modeled atmospheric aerosols in regional  
236 climate simulations with a focus on impacts on the solar resource during the summer season from a  
237 climatic perspective, including projected changes to a medium-range horizon and analysis under  
238 clear-sky conditions. For that we evaluated a set of 20-yr long runs (spanning both present and  
239 future periods) with resolved aerosol-radiation and aerosol-radiation-cloud interactive (two-way)  
240 interactions, on the ground of which we drew original conclusions.

241 In general, the inclusion of interactive aerosols reduces the amount of solar radiation reaching the  
242 surface by a few percent points (~5%) under present climate, as expected (Nabat et al 2015a,  
243 Gutiérrez et al 2018, Pavlidis et al 2020). This effect is larger when the aerosol-cloud interaction  
244 remains turned off, because its activation leads to less cloudiness (over the Mediterranean Europe)  
245 and lower AOD values (over the Atlantic Europe), as evidenced when ACI and ARI simulations  
246 were compared. Differences in RSDS between experiments are in overall well agreement with the  
247 differences found in cloudiness, while they seem to be unlinked with the differences in AOD in  
248 many parts of the domain. In agreement with (Pavlidis et al 2020), AOD plays its major role under  
249 clear-sky conditions. However, the signals supporting its importance under such conditions would  
250 be masked unless coincident dates (at the daily time-scale) are considered. Anyway, differences in  
251 JJA-mean values of RSDS under clear skies between experiments with and without dynamic  
252 aerosols are hardly about 1%, while still significant in some of the southernmost parts of our  
253 European domain, and almost none between ACI and ARI.

254 Regarding the future projections, the patterns for RSDS and those for CCT show again high spatial  
255 correlations in all the GCM and RCM (BASE, ARI and ACI) projections. Although lower, still high  
256 spatial correlations define the matching between the RSDS change patterns and those for AOD in  
257 the GCM and the ARI experiment. GCM, BASE and ARI experiments agree in projecting positive  
258 RSDS change signals in southern and eastern areas (around 5%), while clear differences are found  
259 between the GCM and the BASE or ARI RSDS change patterns (with these two latter being very  
260 similar) in central and northeastern areas, where the positive signals from the GCM turns notably  
261 negative both in BASE and ARI. ACI provides the most singular and negative picture of RSDS  
262 changes among all shown, with widespread decreasing signals of a few percent points, apparently  
263 unlinked to the changes projected in AOD.



264 Previous works (Jerez et al 2015) had already detected inconsistencies in the change signals  
265 between RCM projections and those from their driving GCM, which had been related to the way  
266 aerosols had been represented in the RCM through its impact on the simulated AOD (Bartók et al  
267 2017, Gutiérrez et al 2020, Boé et al 2020), and in particular to the time-evolving aerosols in  
268 scenarios. Our results constitute an example of the impact of cloudiness and AOD in RSDS through  
269 aerosol-related physical mechanisms while keeping unchanged the anthropogenic aerosol emissions  
270 through the simulation period, revealing in this case the prevailing role of CCT changes to explain  
271 RSDS changes, and the capacity of the aerosol-radiation-cloud interactions to significantly alter the  
272 RSDS change patterns (more than what aerosol-radiation interactions alone do). Although change  
273 patterns for RSDS look much more uniform among experiments under clear-sky conditions, the  
274 results presented here may indicate that action-oriented messages from modelling experiments that did  
275 not consider the role of aerosols, in particular in a dynamic way, could be potentially misleading,  
276 thus calling for future research efforts in this line.

### 277 **Author contribution**

278 S. J. conceived this study. L. P.-P., P. J.-G. and J. P. M. designed the experiments and J. M. L.-R.  
279 carried out them. S. J. performed the analysis and prepared the manuscript with contributions from  
280 all co-authors.

### 281 **Acknowledgments**

282 This work is supported by the projects CLIMAX (20642/JLI/18), funded by the Fundación Séneca –  
283 Agencia de Ciencia y Tecnología de la Región de Murcia, EASE (RTI2018-100870-A-I00), funded  
284 by the Spanish Ministry of Science, Innovation and Universities and the European Regional  
285 Development Fund (FEDER), REPAIR (CGL2014-59677-R) and ACEX (CGL2017-87921-R), funded by  
286 the Spanish Ministry of Economy and Competitiveness. S. Jerez has received funding from the *Plan Propio*  
287 *de Investigación* of the University of Murcia (grant No. UMU-2017-10604)

### 288 **Code and data availability**

289 All data and codes used here are available for research purposes by contacting the corresponding author.



## 290 References

- 291 Bartók, B., Wild, M., Folini, D., Lüthi, D., Kotlarski, S., Schär, C., Vautard, R., Jerez, S., & Imecs,  
292 Z. (2017). Projected changes in surface solar radiation in CMIP5 global climate models and in  
293 EURO-CORDEX regional climate models for Europe. *Climate Dynamics*, 49(7-8), 2665-2683.
- 294 Bloomfield, H. C., Brayshaw, D. J., Shaffrey, L. C., Coker, P. J., & Thornton, H. E. (2016).  
295 Quantifying the increasing sensitivity of power systems to climate variability. *Environmental*  
296 *Research Letters*, 11(12).
- 297 Boé, J., Somot, S., Corre, L., & Nabat, P. (2020). Large discrepancies in summer climate change  
298 over Europe as projected by global and regional climate models: causes and consequences. *Climate*  
299 *Dynamics*, 54(5), 2981-3002.
- 300 Boucher, O. (2015). Atmospheric aerosols. In *Atmospheric Aerosols* (pp. 9-24). Springer,  
301 Dordrecht.
- 302 Chapman, E.G., Gustafson, W.I., Easter, R.C., Barnard, J.C., Ghan, S.J., Pekour, M.S., & Fast, J.D.  
303 (2009). Coupling aerosol-cloud-radiative processes in the WRF-Chem model: Investigating the  
304 radiative impact of elevated point sources. *Atmospheric Chemistry and Physics*, 9, 945–964.
- 305 Chen, F., & Dudhia, J. (2001). Coupling an advanced land surface–hydrology model with the Penn  
306 State–NCAR MM5 modeling system. Part I: Model implementation and sensitivity. *Monthly*  
307 *Weather Review*, 129(4), 569-585.
- 308 Chenni, R., Makhlouf, M., Kerbache, T., & Bouzid, A. (2007). A detailed modeling method for  
309 photovoltaic cells. *Energy*, 32(9), 1724-1730.
- 310 Chin, M., Ginoux, P., Kinne, S., Torres, O., Holben, B. N., Duncan, B. N., Martin, R. V., Logan, J.  
311 A., Higurashi, A., & Nakajima, T. (2002). Tropospheric aerosol optical thickness from the  
312 GOCART model and comparisons with satellite and Sun photometer measurements. *Journal of the*  
313 *Atmospheric Sciences*, 59, 461 – 483.



- 314 Collins, S., Deane, P., Gallachóir, B. Ó., Pfenninger, S., & Staffell, I. (2018). Impacts of inter-  
315 annual wind and solar variations on the European power system. *Joule*, 2(10), 2076-2090.
- 316 Croft, B., Pierce, J. R., Martin, R. V., Hoose, C., & Lohmann, U. (2012). Uncertainty associated  
317 with convective wet removal of entrained aerosols in a global climate model. *Atmospheric*  
318 *Chemistry and Physics*, 12(22), 10725-10748.
- 319 Crook, J. A., Jones, L. A., Forster, P. M., & Crook, R. (2011). Climate change impacts on future  
320 photovoltaic and concentrated solar power energy output. *Energy & Environmental Science*, 4(9),  
321 3101-3109.
- 322 Dubey, S., Sarvaiya, J. N., & Seshadri, B. (2013). Temperature dependent photovoltaic (PV)  
323 efficiency and its effect on PV production in the world—a review. *Energy Procedia*, 33, 311-321.
- 324 Fast, J. D., Gustafson Jr, W. I., Easter, R. C., Zaveri, R. A., Barnard, J. C., Chapman, E. G., Grell, G.  
325 A., & Peckham, S. E. (2006). Evolution of ozone, particulates, and aerosol direct radiative forcing  
326 in the vicinity of Houston using a fully coupled meteorology chemistry aerosol model. *Journal of*  
327 *Geophysical Research: Atmospheres*, 111(D21).
- 328 Gaetani, M., Huld, T., Vignati, E., Monforti-Ferrario, F., Dosio, A., & Raes, F. (2014). The near  
329 future availability of photovoltaic energy in Europe and Africa in climate-aerosol modeling  
330 experiments. *Renewable and Sustainable Energy Reviews*, 38, 706-716.
- 331 Geiger, H., Barnes, I., Bejan, I., Benter, T., & Spittler, M. (2003). The tropospheric degradation of  
332 isoprene: an updated module for the regional atmospheric chemistry mechanism. *Atmospheric*  
333 *Environment*, 37, 1503 - 1519.
- 334 Germer, S., & Kleidon, A. (2019). Have wind turbines in Germany generated electricity as would be  
335 expected from the prevailing wind conditions in 2000-2014?. *PloS One*, 14(2), e0211028.
- 336 Gil, V., Gaertner, M. A., Gutierrez, C., & Losada, T. (2019). Impact of climate change on solar  
337 irradiation and variability over the Iberian Peninsula using regional climate models. *International*  
338 *Journal of Climatology*, 39(3), 1733-1747.



- 339 Ginoux, P., Chin, M., Tegen, I., Prospero, J. M., Holben, B., Dubovik, O., & Lin, S. J. (2001).  
340 Sources and distributions of dust aerosols simulated with the GOCART model. *Journal of*  
341 *Geophysical Research: Atmospheres*, 106(D17), 20255-20273.
- 342 Giorgetta, M., Jungclaus, J., Reick, C., Legutke, S., Brovkin, V., Crueger, T., Esch, M., Fieg, K.,  
343 Glushak, K., Gayler, V., Haak, H., Hollweg, H.-D., Kinne, S., Kornblueh, L., Matei, D., Mauritsen,  
344 T., Mikolajewicz, U., Müller, W., Notz, D., Raddatz, T., Rast, S., Roeckner, E., Salzmann, M.,  
345 Schmidt, H., Schnur, R., Segschneider, J., Six, K., Stockhause, M., Wegner, J., Widmann, H.,  
346 Wieners, K.-H., Claussen, M., Marotzke, J., & Stevens, B. (2012a). Forcing Data for Regional  
347 Climate Models Based on the MPI-ESM-LR Model of the Max Planck Institute for Meteorology  
348 (MPI-M): The CMIP5 Historical Experiment, World Data Center for Climate (WDCC) at DKRZ,  
349 [https://doi.org/10.1594/WDCC/RCM\\_CMIP5\\_historical-LR](https://doi.org/10.1594/WDCC/RCM_CMIP5_historical-LR).
- 350 Giorgetta, M., Jungclaus, J., Reick, C., Legutke, S., Brovkin, V., Crueger, T., Esch, M., Fieg, K.,  
351 Glushak, K., Gayler, V., Haak, H., Hollweg, H.-D., Kinne, S., Kornblueh, L., Matei, D., Mauritsen,  
352 T., Mikolajewicz, U., Müller, W., Notz, D., Raddatz, T., Rast, S., Roeckner, E., Salzmann, M.,  
353 Schmidt, H., Schnur, R., Segschneider, J., Six, K., Stockhause, M., Wegner, J., Widmann, H.,  
354 Wieners, K.-H., Claussen, M., Marotzke, J., and Stevens, B. (2012b). Forcing data for Regional  
355 Climate Models Based on the MPI-ESM-LR model of the Max Planck Institute for Meteorology  
356 (MPI-M): The CMIP5rcp85 experiment, World Data Center for Climate (WDCC) at DKRZ, [https://](https://doi.org/10.1594/WDCC/RCM_CMIP5_rcp85-LR)  
357 [doi.org/10.1594/WDCC/RCM\\_CMIP5\\_rcp85-LR](https://doi.org/10.1594/WDCC/RCM_CMIP5_rcp85-LR).
- 358 Giorgi, F., Bi, X., & Qian, Y. (2002). Direct radiative forcing and regional climatic effects of  
359 anthropogenic aerosols over East Asia: A regional coupled climate chemistry/aerosol model study.  
360 *Journal of Geophysical Research: Atmospheres*, 107(D20), AAC-7.
- 361 Guenther, A., Karl, T., Harley, P., Wiedinmyer, C., Palmer, P. I., & Geron, C. (2006). Estimates of  
362 global terrestrial isoprene emissions using MEGAN (Model of Emissions of Gases and Aerosols  
363 from Nature). *Atmospheric Chemistry and Physics*, 6(11), 3181-3210.
- 364 Gutiérrez, C., Somot, S., Nabat, P., Mallet, M., Gaertner, M. Á., & Perpiñán, O. (2018). Impact of  
365 aerosols on the spatiotemporal variability of photovoltaic energy production in the Euro-  
366 Mediterranean area. *Solar Energy*, 174, 1142-1152.



- 367 Gutiérrez, C., Somot, S., Nabat, P., Mallet, M., Corre, L., van Meijgaard, E., Perpiñán, O., &  
368 Gaertner, M. Á. (2020). Future evolution of surface solar radiation and photovoltaic potential in  
369 Europe: investigating the role of aerosols. *Environmental Research Letters*, 15(3), 034035.
- 370 Grell, G. A. (1993). Prognostic evaluation of assumptions used by cumulus parameterizations.  
371 *Monthly Weather Review*, 121(3), 764-787.
- 372 Grell, G. A., & Dévényi, D. (2002). A generalized approach to parameterizing convection  
373 combining ensemble and data assimilation techniques. *Geophysical Research Letters*, 29(14), 38-1.
- 374 Grell, G. A., Peckham, S. E., Schmitz, R., McKeen, S. A., Frost, G., Skamarock, W. C., & Eder, B.  
375 (2005). Fully coupled “online” chemistry within the WRF model. *Atmospheric Environment*,  
376 39(37), 6957-6975.
- 377 Hong, S. Y., Noh, Y., & Dudhia, J. (2006). A new vertical diffusion package with an explicit  
378 treatment of entrainment processes. *Monthly weather review*, 134(9), 2318-2341.
- 379 Iacono, M. J., Delamere, J. S., Mlawer, E. J., Shephard, M. W., Clough, S. A., & Collins, W. D.  
380 (2008). Radiative forcing by long lived greenhouse gases: Calculations with the AER radiative  
381 transfer models. *Journal of Geophysical Research: Atmospheres*, 113(D13).
- 382 IPCC (2013). *Climate Change 2013: The Physical Science Basis. Contribution of Working Group I*  
383 *to the Fifth Assessment Report of the Intergovernmental Panel on Climate Change.* T. F. Stocker, D.  
384 Qin, G.-K. Plattner, M. Tignor, S. K. Allen, J. Boschung, A. Nauels, Y. Xia, V. Bex and P. M.  
385 Midgley (eds.). Cambridge University Press, Cambridge, United Kingdom and New York, NY,  
386 USA, 1535 pp.
- 387 IPCC (2014). *Climate Change 2014: Mitigation of Climate Change. Contribution of Working Group*  
388 *III to the Fifth Assessment Report of the Intergovernmental Panel on Climate Change.* O.  
389 Edenhofer, R. Pichs-Madruga, Y. Sokona, E. Farahani, S. Kadner, K. Seyboth, A. Adler, I. Baum, S.  
390 Brunner, P. Eickemeier, B. Kriemann, J. Savolainen, S. Schlömer, C. von Stechow, T. Zwickel and  
391 J.C. Minx (eds.). Cambridge University Press, Cambridge, United Kingdom and New York, NY,  
392 USA.



- 393 IRENA (2019). Global energy transformation: A roadmap to 2050 (2019 edition). International  
394 Renewable Energy Agency, Abu Dhabi.
- 395 Jacob, D., Petersen, J., Eggert, B., Alias, A., Christensen, O. B., Bouwer, L. M., et al. (2014).  
396 EURO-CORDEX: new high-resolution climate change projections for European impact research.  
397 *Regional environmental change*, 14(2), 563-578.
- 398 Jacob, D., Teichmann, C., Sobolowski, S., Katragkou, E., Anders, I., Belda, M., et al. (2020).  
399 Regional climate downscaling over Europe: perspectives from the EURO-CORDEX community.  
400 *Regional Environmental Change*, 20(2).
- 401 Jerez, S., Trigo, R. M., Vicente-Serrano, S. M., Pozo-Vázquez, D., Lorente-Plazas, R., Lorenzo-  
402 Lacruz, J., Santos-Alamillos, F., & Montávez, J. P. (2013). The impact of the North Atlantic  
403 Oscillation on renewable energy resources in southwestern Europe. *Journal of Applied Meteorology*  
404 *and Climatology*, 52(10), 2204-2225.
- 405 Jerez, S., Tobin, I., Vautard, R., Montávez, J. P., López-Romero, J. M., Thais, F., Bartok, B.,  
406 Christensen, O. B., Colette, A., Déqué, M., Nikulin, G., Kotlarski, S., van Meijgaard, E., teichmann,  
407 C., & Wild, M. (2015). The impact of climate change on photovoltaic power generation in Europe.  
408 *Nature Communications*, 6, 10014.
- 409 Jerez, S., López-Romero, J. M., Turco, M., Jiménez-Guerrero, P., Vautard, R., & Montávez, J. P.  
410 (2018). Impact of evolving greenhouse gas forcing on the warming signal in regional climate model  
411 experiments. *Nature Communications*, 9(1), 1304.
- 412 Jerez, S., Tobin, I., Turco, M., Jiménez-Guerrero, P., Vautard, R., & Montávez, J. P. (2019). Future  
413 changes, or lack thereof, in the temporal variability of the combined wind-plus-solar power  
414 production in Europe. *Renewable Energy*, 139, 251-260.
- 415 Kinne, S. (2019). Aerosol radiative effects with MACv2. *Atmospheric Chemistry and Physics*,  
416 19(16), 10919-10959.



- 417 Kloster, S., Dentener, F., Feichter, J., Raes, F., Lohmann, U., Roeckner, E., & Fischer-Bruns, I.  
418 (2010). A GCM study of future climate response to aerosol pollution reductions. *Climate Dynamics*,  
419 34(7-8), 1177-1194.
- 420 Kozarcenin, S., Andresen, G. B., & Greiner, M. (2018). Impact of Climate Change on the Backup  
421 Infrastructure of Highly Renewable Electricity Systems. *Journal of Sustainable Development of*  
422 *Energy, Water and Environment Systems*, 6(4), 710-724.
- 423 Lamarque, J. F., Bond, T. C., Eyring, V., Granier, C., Heil, A., Klimont, Z., et al. (2010). Historical  
424 (1850–2000) gridded anthropogenic and biomass burning emissions of reactive gases and aerosols:  
425 methodology and application. *Atmospheric Chemistry and Physics*, 10(15), 7017-7039.
- 426 Li, X., Wagner, F., Peng, W., Yang, J., & Mauzerall, D. L. (2017). Reduction of solar photovoltaic  
427 resources due to air pollution in China. *Proceedings of the National Academy of Sciences*, 114(45),  
428 11867-11872.
- 429 Lin, Y. L., Farley, R. D., & Orville, H. D. (1983). Bulk parameterization of the snow field in a cloud  
430 model. *Journal of Climate and Applied Meteorology*, 22(6), 1065-1092.
- 431 Moss, R. H., Edmonds, J. A., Hibbard, K. A., Manning, M. R., Rose, S. K., Van Vuuren, D. P., et al.  
432 (2010). The next generation of scenarios for climate change research and assessment. *Nature*,  
433 463(7282), 747.
- 434 Müller, J., Folini, D., Wild, M., & Pfenninger, S. (2019). CMIP-5 models project photovoltaics are a  
435 no-regrets investment in Europe irrespective of climate change. *Energy*, 171, 135-148.
- 436 Nabat, P., Somot, S., Mallet, M., Sanchez Lorenzo, A., & Wild, M. (2014). Contribution of  
437 anthropogenic sulfate aerosols to the changing Euro Mediterranean climate since 1980.  
438 *Geophysical Research Letters*, 41(15), 5605-5611.
- 439 Nabat, P., Somot, S., Mallet, M., Sevault, F., Chiacchio, M., & Wild, M. (2015a). Direct and semi-  
440 direct aerosol radiative effect on the Mediterranean climate variability using a coupled regional  
441 climate system model. *Climate Dynamics*, 44(3-4), 1127-1155.





- 442 Nabat, P., Somot, S., Mallet, M., Michou, M., Sevault, F., Driouech, F., Meloni, D., di Sarra, G., di  
443 Biagio, C., Formenti, P., Sicard, M., Leon, J. F. & Bouin, M. N. (2015b). Dust aerosol radiative  
444 effects during summer 2012 simulated with a coupled regional aerosol–atmosphere–ocean model  
445 over the Mediterranean. *Atmospheric Chemistry and Physics*, 15(6), 3303-3326.
- 446 Palacios-Peña, L., Lorente-Plazas, R., Montávez, J. P. and Jiménez-Guerrero, P. (2019a) Saharan  
447 Dust Modeling Over the Mediterranean Basin and Central Europe: Does the Resolution Matter?.  
448 *Frontiers in Earth Science*, 7, 290.
- 449 Palacios-Peña, L., Jiménez-Guerrero, P., Baró, R., Balzarini, A., Bianconi, R., Curci, G., Landi, T.  
450 C., Pirovano, G., Prank, M., Riccio, A., Tuccella, P., & Galmarini, S. (2019b). Aerosol optical  
451 properties over Europe: an evaluation of the AQMEII Phase 3 simulations against satellite  
452 observations. *Atmospheric Chemistry and Physics*, 19(5), 2965-2990.
- 453 Palacios-Peña, L., Montávez, J.P., López-Romero, J.M., Jerez, S., Gómez-Navarro, J.J., Lorente-  
454 Plazas, R., Ruiz, J., & Jiménez-Guerrero, P. (2020). Added Value of Aerosol-Cloud Interactions for  
455 Representing Aerosol Optical Depth in an Online Coupled Climate-Chemistry Model over Europe.  
456 *Atmosphere*, 11, 360.
- 457 Pavlidis, V., Katragkou, E., Prein, A., Georgoulas, A. K., Kartsios, S., Zanis, P., & Karacostas, T.  
458 (2020). Investigating the sensitivity to resolving aerosol interactions in downscaling regional model  
459 experiments with WRFv3.8.1 over Europe. *Geoscience Model Development*, 13, 2511–2532
- 460 Ravestein, P., van der Schrier, G., Haarsma, R., Scheele, R., & van den Broek, M. (2018).  
461 Vulnerability of European intermittent renewable energy supply to climate change and climate  
462 variability. *Renewable and Sustainable Energy Reviews*, 97, 497-508.
- 463 Rohrig, K., Berkhout, V., Callies, D., Durstewitz, M., Faulstich, S., Hahn, B., et al. (2019).  
464 Powering the 21st century by wind energy – Options, facts, figures. *Applied Physics Reviews*, 6(3),  
465 031303.
- 466 Rummukainen, M. (2010). State of the art with regional climate models. *Wiley Interdisciplinary*  
467 *Reviews: Climate Change*, 1(1), 82-96.



468 Ruti, P. M., Somot, S., Giorgi, F., Dubois, C., Flaounas, E., Obermann, A., et al. (2016). MED-  
469 CORDEX initiative for Mediterranean climate studies. *Bulletin of the American Meteorological*  
470 *Society*, 97(7), 1187-1208.

471 Rutledge, S. A., & Hobbs, P. V. (1984). The Mesoscale and Microscale Structure and Organization  
472 of Clouds and Precipitation in Midlatitude Cyclones. XII: A Diagnostic Modeling Study of  
473 Precipitation Development in Narrow Cold-Frontal Rainbands. *Journal of Atmospheric Science*, 41,  
474 2949–2972.

475 Schewe, J., Gosling, S. N., Reyer, C., Zhao, F., Ciais, P., Elliott, J., Francois, L., Huber, V., Lotze,  
476 H. K., Seneviratne, S. I., van Vliet, M. T. H., Vautard, R., Wada, Y., Breuer, L., Büchner, M.,  
477 Carozza, D. A., Chang, J., Coll, M., Deryng, D., de Wit, A., Eddy, T. D., Folberth, C., Frieler, K.,  
478 Friend, A. D., Gerten, D., Gudmundsson, L., Hanasaki, N., Ito, A., Khabarov, N., Kim, H.,  
479 Lawrence, P., Morfopoulos, C., Müller, C., Schmied, H. M., Orth, R., Ostberg, S., Pokhrel, Y.,  
480 Pugh, T. A. M., Sakurai, G., Satoh, Y., Schmid, E., Stacke, T., Steenbeek, J., Steinkamp, J., Tang,  
481 Q., Tian, H., Tittensor, D.P., Volkholz, J., Wang, X., & Warszawski, L. (2019). State-of-the-art  
482 global models underestimate impacts from climate extremes. *Nature Communications*, 10(1), 1005.

483 Schlott, M., Kies, A., Brown, T., Schramm, S., & Greiner, M. (2018). The impact of climate change  
484 on a cost-optimal highly renewable European electricity network. *Applied Energy*, 230, 1645-1659.

485 Seinfeld, J. H., Bretherton, C., Carslaw, K. S., Coe, H., DeMott, P. J., Dunlea, E. J., et al. (2016).  
486 Improving our fundamental understanding of the role of aerosol– cloud interactions in the climate  
487 system. *Proceedings of the National Academy of Sciences*, 113(21), 5781-5790.

488 Skamarock, W. C., Klemp, J. B., Dudhia, J., Gill, D. O., Barker, D. M., Wang, W., & Powers, J. G.  
489 (2008). A description of the Advanced Research WRF version 3. Technical report, NCAR Tech.  
490 Note TN-475+STR, doi:10.5065/D68S4MVH.

491 Soares, P. M., Brito, M. C., & Careto, J. A. (2019). Persistence of the high solar potential in Africa  
492 in a changing climate. *Environmental Research Letters*.

493 Solaun, K., & Cerdá, E. (2019). Climate change impacts on renewable energy generation. A review  
494 of quantitative projections. *Renewable and Sustainable Energy Reviews*, 116, 109415.



- 495 Stockwell, W. R., Kirchner, F., Kuhn, M., & Seefeld, S. (1997). A new mechanism for regional  
496 atmospheric chemistry modeling. *Journal of Geophysical Research: Atmospheres*, 102, 25 847 - 25  
497 879.
- 498 Taylor, K. E., Stouffer, R. J., & Meehl, G. A. (2012). An overview of CMIP5 and the experiment  
499 design. *Bulletin of the American Meteorological Society*, 93(4), 485-498.
- 500 Tewari, M., Chen, F., Wang, W., Dudhia, J., LeMone, M. A., Mitchell, K., Ek, M., Gayno, G.,  
501 Wegiel, J. W., & Cuenca, R. H. (2004, January). Implementation and verification of the unified  
502 NOAA land surface model in the WRF model. In 20th conference on weather analysis and  
503 forecasting/16th conference on numerical weather prediction (Vol. 1115). Seattle, WA: American  
504 Meteorological Society.
- 505 Tobin, I., Vautard, R., Balog, I., Bréon, F. M., Jerez, S., Ruti, P. M., Thais, F., Vrac, M., & Yiou, P.  
506 (2015). Assessing climate change impacts on European wind energy from ENSEMBLES high-  
507 resolution climate projections. *Climatic Change*, 128(1-2), 99-112.
- 508 Tobin, I., Jerez, S., Vautard, R., Thais, F., Van Meijgaard, E., Prein, A., Déqué, M., Kotlarski, S.,  
509 Maule, C. F., & Nikulin, G. (2016). Climate change impacts on the power generation potential of a  
510 European mid-century wind farms scenario. *Environmental Research Letters*, 11(3), 034013.
- 511 Tobin, I., Greuell, W., Jerez, S., Ludwig, F., Vautard, R., Van Vliet, M. T. H., & Bréon, F. M. (2018).  
512 Vulnerabilities and resilience of European power generation to 1.5 C, 2 C and 3 C warming.  
513 *Environmental Research Letters*, 13(4), 044024.
- 514 Troccoli, A., Goodess, C., Jones, P., Penny, L., Dorling, S., Harpham, C., et al. (2018). Creating a  
515 proof-of-concept climate service to assess future renewable energy mixes in Europe: An overview  
516 of the C3S ECEM project. *Advances in Science and Research*, 15, 191-205.
- 517 Turner, S. W., Voisin, N., Fazio, J., Hua, D., & Jourabchi, M. (2019). Compound climate events  
518 transform electrical power shortfall risk in the Pacific Northwest. *Nature Communications*, 10(1), 8.



- 519 van der Wiel, K., Bloomfield, H. C., Lee, R. W., Stoop, L. P., Blackport, R., Screen, J. A., & Selten,  
520 F. M. (2019). The influence of weather regimes on European renewable energy production and  
521 demand. *Environmental Research Letters*, *14*(9), 094010.
- 522 van Ruijven, B. J., De Cian, E., & Wing, I. S. (2019). Amplification of future energy demand  
523 growth due to climate change. *Nature Communications*, *10*(1), 2762.
- 524 Wang, H., Xie, S. P., Tokinaga, H., Liu, Q., & Kosaka, Y. (2016). Detecting cross equatorial wind  
525 change as a fingerprint of climate response to anthropogenic aerosol forcing. *Geophysical Research*  
526 *Letters*, *43*(7), 3444-3450.
- 527 Wilcox, L. J., Highwood, E. J., & Dunstone, N. J. (2013). The influence of anthropogenic aerosol  
528 on multi-decadal variations of historical global climate. *Environmental Research Letters*, *8*(2),  
529 024033.
- 530 Wild, M., Folini, D., Henschel, F., Fischer, N., & Müller, B. (2015). Projections of long-term  
531 changes in solar radiation based on CMIP5 climate models and their influence on energy yields of  
532 photovoltaic systems. *Solar Energy*, *116*, 12-24.
- 533 Wild, O., Zhu, X., Prather, M. J., & Fast, J. (2002). Accurate Simulation of In- and Below-Cloud  
534 Photolysis in Tropospheric Chemical Models. *Journal of Atmospheric Chemistry*, *37*, 245 – 282.
- 535 Zappa, W., Junginger, M., & van den Broek, M. (2019). Is a 100% renewable European power  
536 system feasible by 2050?. *Applied Energy*, *233*, 1027-1050.



537 **Figure caption**

538 **Figure 1.** Relative differences between the WRF simulations in the RSDS (a to c), CCT (d to f) and  
539 AOD at 550 nm (g to i) summer (JJA) climatologies in the present period (1991-2010), squared if  
540 statistically significant ( $p < 0.05$ ); units: %. Note that panels g and h are referred to the horizontal  
541 colorbar just below them and simply represent the AOD summer climatologies in ARI and ACI  
542 respectively. Spatial correlations ( $s\_corr$ ) between the patterns in the second and third rows and the  
543 respective patterns in the first row are indicated in the headers.

544 **Figure 2.** Relative differences between the WRF simulations in the  $RSDS_{cs}$  (a to c) and  $AOD_{cs}$  at  
545 550 nm (d to f) summer (JJA) climatologies, this is under clear-sky conditions, in the present period  
546 (1991-2010), squared if statistically significant ( $p < 0.05$ ); units: %. Note that panels d and e are  
547 referred to the horizontal colorbar just below them and simply represent the AOD summer  
548 climatologies in ARI and ACI respectively. Gray shaded areas depict grid point where less than 75%  
549 of the summer mean values in the time series of  $RSDS_{cs}$  and  $AOD_{cs}$  were not missing values. Spatial  
550 correlations ( $s\_corr$ ) between the patterns in the second row and the respective patterns in the first  
551 row are indicated in the headers.

552 **Figure 3.** Projected changes for the RSDS (a to d), CCT (e to h) and AOD at 550nm (i to l) summer  
553 (JJA) climatologies by the GCM (first column) and the WRF experiments (second to fourth  
554 columns); units: %. Squares highlight statistically significant signals ( $p < 0.05$ ). Note that panel i is  
555 referred to the horizontal colorbar just below it. Spatial correlations ( $s\_corr$ ) between the patterns in  
556 the second and third rows and the respective patterns in the first row are indicated in the headers.

557 **Figure 4.** Projected changes for the  $RSDS_{cs}$  (a to c) and  $AOD_{cs}$  at 550nm (d to f) summer (JJA)  
558 climatologies, this is under clear-sky conditions, by the WRF experiments, squared if statistically  
559 significant ( $p < 0.05$ ); units: %. Gray shaded areas depict grid point where less than 75% of the  
560 summer mean values in the time series of  $RSDS_{cs}$  and  $AOD_{cs}$  were not missing values in both the  
561 present and the future period. Spatial correlations ( $s\_corr$ ) between the patterns in the second row  
562 and the respective patterns in the first row are indicated in the headers.



### RSDS, CCT & AOD JJA climatologies for 1991-2010: differences between experiments

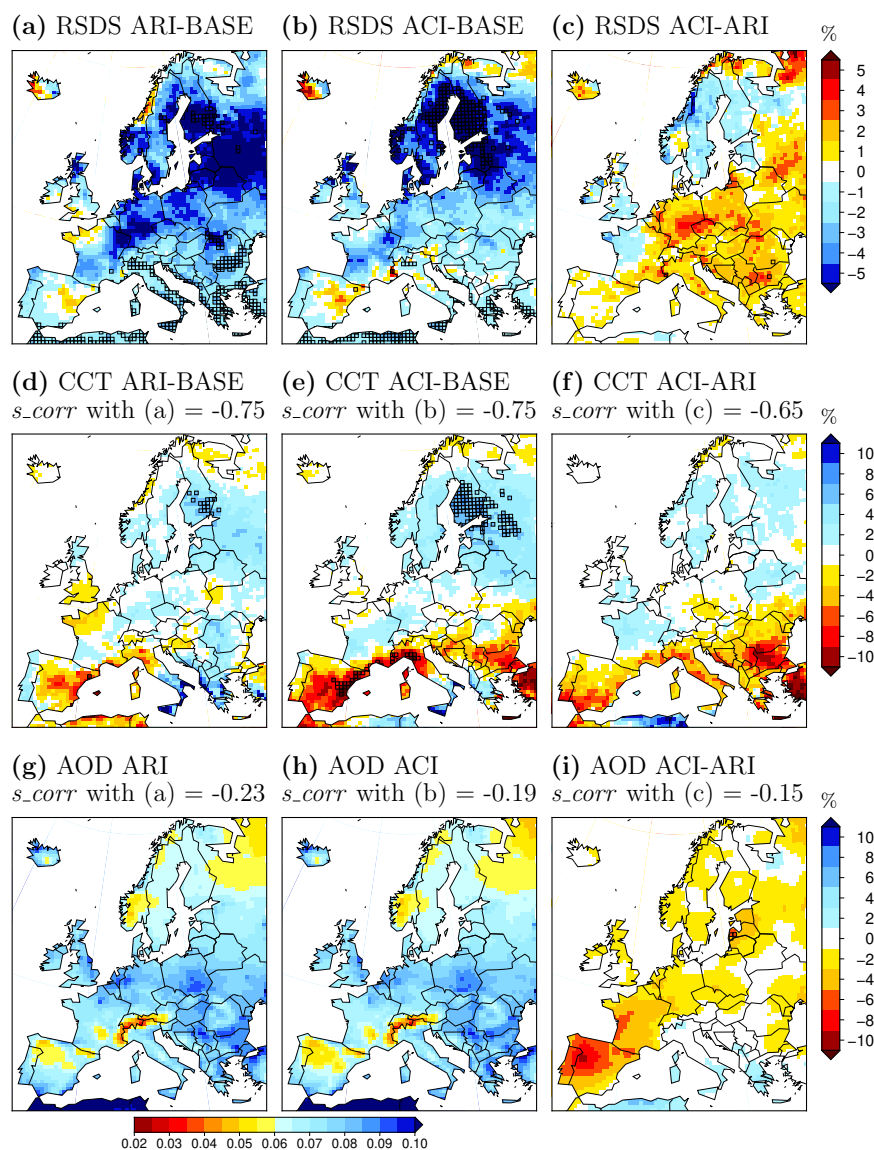


Figure 1



### RSDS<sub>cs</sub> & AOD<sub>cs</sub> JJA climatologies for 1991-2010: differences between experiments

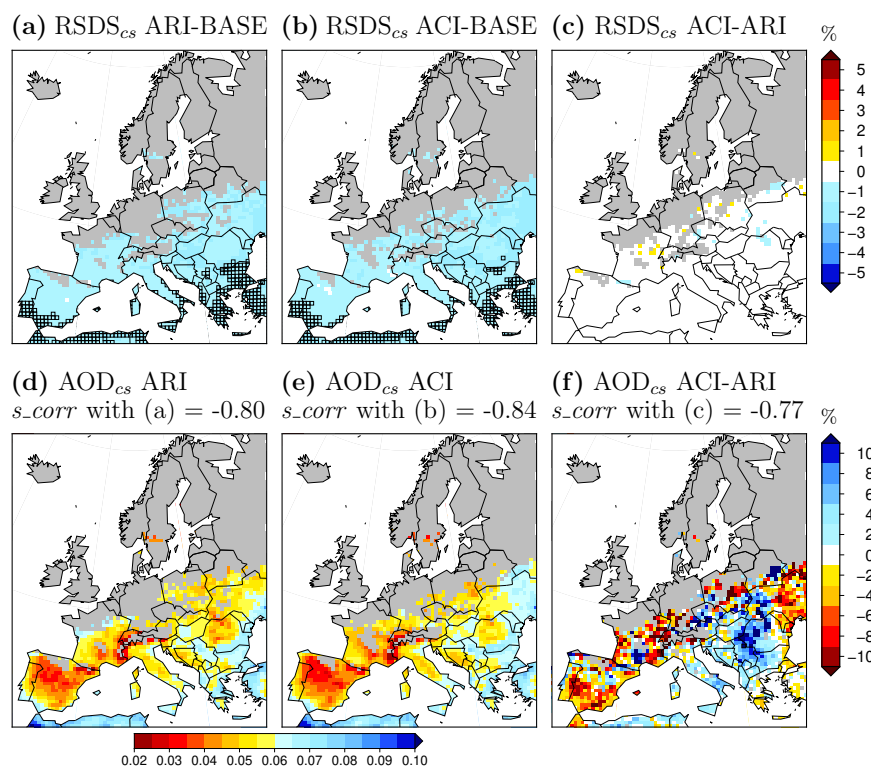


Figure 2



### RSDS, CCT & AOD JJA changes (2031-2050 vs. 1991-2010)

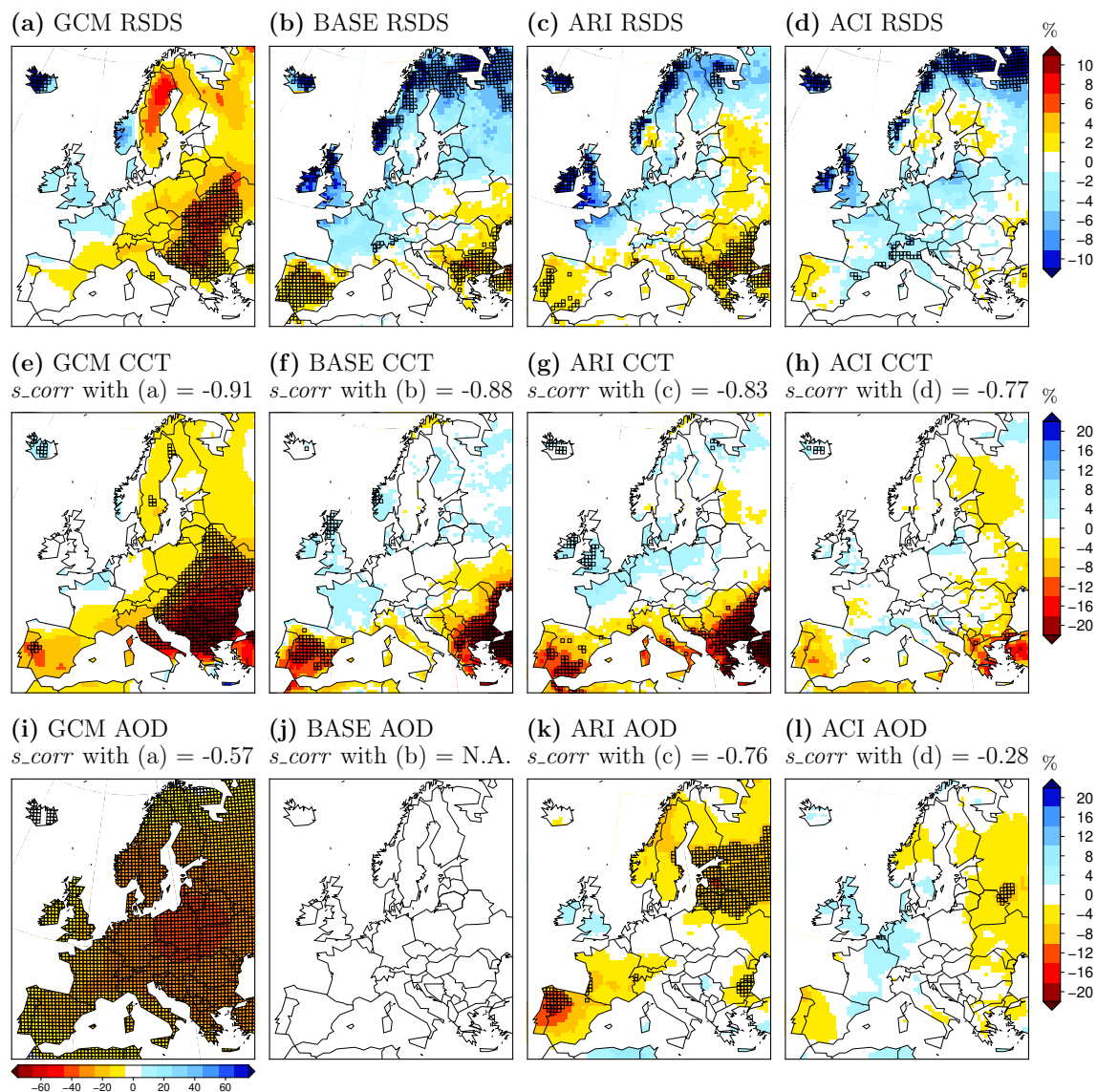


Figure 3





### RSDS<sub>cs</sub> & AOD<sub>cs</sub> JJA changes (2031-2050 vs. 1991-2010)

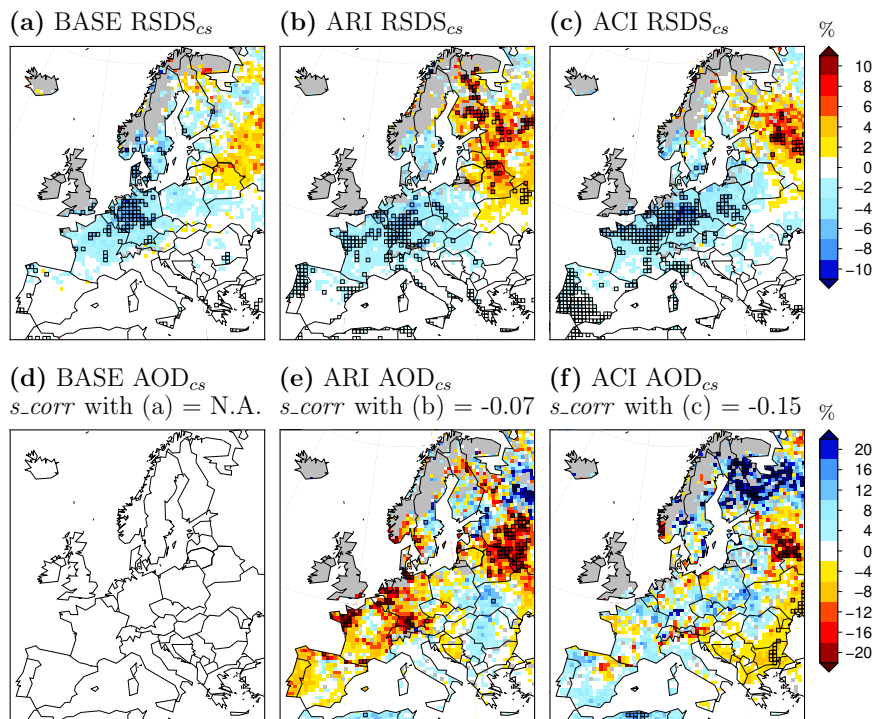


Figure 4